1 Contact Dynamics for Beginners

L. Brendel, T. Unger, D. E. Wolf

Institut für Physik, Universität Duisburg-Essen, D-47048 Duisburg, Germany.

1.1 Introduction

For the dynamical properties of dense granular media, where lasting contacts dominate, steric hindrance and solid friction play a crucial role. Examples are the withdrawal of material from a silo, the compaction of powders, imprinting of one's foot on a beach, or the stability of an ancient vault in an earthquake. For sufficiently rigid materials elastic or plastic deformation of the particles can be so small in these processes that they can be safely neglected. What matters is the rearrangement of rigid particles. Contact Dynamics is a simulation method that was developed to deal with rigid, frictional particles. The purpose of this article is threefold: It contains a description of the Contact Dynamics simulation method, it discusses when this method is more efficient than Molecular Dynamics, and finally it describes how the basic algorithm can be extended to simulate cohesive powders. In the first two parts cohesion is largely considered to be negligible, but this is not true for fine powders (particle diameters of about $1\mu m$ and smaller), nor for wet sand.

Contact Dynamics (CD) is a discrete element method like Molecular Dynamics (MD), i.e. the equations of motion are integrated for each particle. However, by considering the particles as perfectly rigid, contact dynamics suppresses phenomena caused by particle deformation. It represents the deformation of the granular medium as a whole in an idealized way exclusively by particle rearrangements. Obviously the volume exclusion of perfectly rigid particles is a constraint that is formulated as an inequality: The distance between the particle surfaces ("gap") must be larger or equal zero. Such constraints are called unilateral. They are only active if the gap is zero, and otherwise have no effect. Therefore the number of degrees of freedom in the system depends on the number of contacts (more precisely: active constraints) and is itself a dynamical variable, which explains the name "Contact Dynamics". By contrast, in soft particle MD as well as in event driven MD the number of degrees of freedom does not change in time.

Imposing constraints requires implicit forces (constraint forces) which cannot be calculated from the positions and velocities of the particles alone. The constraint forces are determined such as to compensate all forces that would cause constraint-violating accelerations.

The volume exclusion constraint allows only complementary values of gap g and constraint force $\mathcal{R}_n$, which is normal to the tangent surface at the contact point: Their product must be zero, $g\mathcal{R}_n = 0$. This is expressed by the Signorini graph, on the left of Fig. 1.1. As long as $g > 0$ the constraint is not active, hence $\mathcal{R}_n = 0$. If $g = 0$, the constraint force must prevent interpenetration of the particles. Hence it must be repulsive and can take whatever
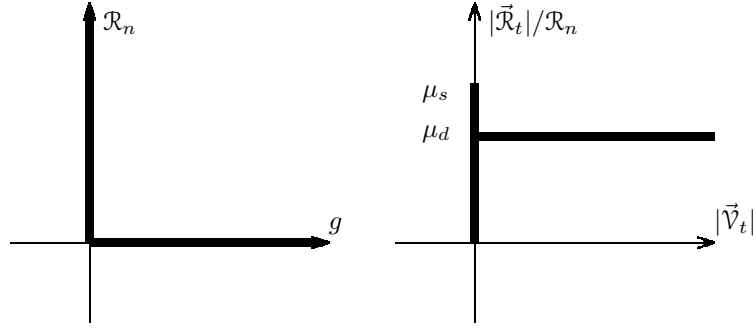
Figure 1.1: Volume exclusion constraint (left): Gap g and constraint force $\mathcal{R}_n$ are complementary to each other (Signorini graph). Non-sliding constraint (right): The constraint force (static friction force) plus the sliding friction force constitute the Coulomb graph. In this paper the static and dynamic friction coefficients are assumed to be equal, $\mu_s = \mu_d = \mu$.

non-negative value is needed for this purpose.

In addition to volume exclusion we have to deal with a second type of constraint, the non-sliding constraint of frictional contacts. It is only active, if the tangential relative velocity $|\vec{\mathcal{V}}_t|$ is zero. In this case the static friction force can be nonzero and assumes whatever tangential direction and value $0 \leq |\vec{\mathcal{R}}_t| \leq \mu_s \mathcal{R}_n$ are needed to prevent sliding. If a constraint force outside this Coulomb cone would be needed, sliding cannot be avoided, and one obtains $\vec{\mathcal{V}}_t \neq 0$ and the well defined sliding friction $-\mu_d \mathcal{R}_n \vec{\mathcal{V}}_t / |\vec{\mathcal{V}}_t|$. The absolute values of the tangential velocity and the friction force lie on the Coulomb graph (right hand side of Fig. 1.1).

Although both graphs have infinitely steep parts they can be implemented in the CD method without any change, in contrast to MD. The CD technique can handle rigid particles and static frictional contacts without regularizing the graphs, Fig. 1.1. Hence it is able to overcome some difficulties that arise in soft particle molecular dynamics (MD) (see Stefan Luding's contribution in this book) or in event driven simulations [11, 17].

Algorithms for contact dynamics were already developed in the 1980-ies [16, 1]. In the context of granular media they were made known to a wider physics community by Jean and Moreau [13, 18, 12]. Two recent reviews were given by Schwager and Pöschel [24] and by Unger and Kertész [26]. The following sections closely follow the presentation given in [25, 26].

1.2   Discrete dynamical equations

Collisions of rigid particles give rise to discontinuous velocities during the time-evolution. In such non-smooth mechanics the use of second or higher order schemes for the numerical integration of the motion is not beneficial and could even be problematic. Therefore first order

schemes are applied, e.g. an implicit Euler integration in our CD code:

$$\vec{v}_i\,(t+\Delta t) \;=\; \vec{v}_i\,(t) + \frac{1}{m_i}\vec{F}_i\,(t+\Delta t)\,\Delta t\,. \tag{1.1}$$

$$\vec{r}_i\,(t+\Delta t) \;=\; \vec{r}_i\,(t) + \vec{v}_i\,(t+\Delta t)\,\Delta t \tag{1.2}$$

The two equations describe the change of velocity and center of mass position during one time step for the ith particle. The vector $\vec{F}_i$ denotes the sum of the forces acting on the particle and is calculated in each step such that the constraints remain fulfilled.

The time-stepping is similar for the rotational degrees of freedom: The orientation of a particle is updated with the new angular velocity $\vec{\omega}_i\,(t+\Delta t)$, while for the update of $\vec{\omega}_i$ we use the torque $\vec{T}_i\,(t+\Delta t)$ exerted by the contact forces.

1.3   Volume exclusion in a one-dimensional example

Before we describe the three dimensional implementation of contact dynamics, the structure of the algorithm shall be explained with the simplest possible example, the central collision of two non-rotating equal spheres, labeled $i = 1$ or 2, with zero restitution coefficient (see Fig. 1.2). In this one-dimensional example only the volume exclusion constraint occurs, and the constraint force has only one component, $\mathcal{R}$.

As the particles only interact, if they are in contact, it is important to keep a list of existing and incipient contacts, i.e. contacts that may form during the next time step. With each of these contacts one can associate a relative velocity $\mathcal{V} = dg/dt$ which is zero for closed contacts, negative for incipient contacts, and positive for particles that move away from each other.

For the one-dimensional example it is trivial to connect the contact-related quantities, $\mathcal{V}$ and $\mathcal{R}$, to the particle velocities v_1 and v_2 and the interaction forces R_1 and R_2 experienced by the particles:

$$\mathcal{V} = v_2 - v_1 \;=\; (-1,1)\cdot\begin{pmatrix} v_1 \\ v_2 \end{pmatrix}, \tag{1.3}$$

$$\begin{pmatrix} R_1 \\ R_2 \end{pmatrix} \;=\; \begin{pmatrix} -1 \\ 1 \end{pmatrix}\mathcal{R}\,. \tag{1.4}$$

Eq. (1.4) is simply the action-reaction principle.

In three dimensions, the relative velocity $\vec{\mathcal{V}}$ and the constraint force $\vec{\mathcal{R}}$ have a normal as well as tangential components for each contact. We shall see below that they are related to the velocities and angular velocities, respectively the interaction forces and torques by a straigthforward generalization of the linear relations (1.3) and (1.4).

Newton's equation of motion relates the particle acceleration to the sum of the interaction force R_i and a possible external force F_i^{ext}:

$$\frac{d}{dt}\begin{pmatrix} v_1 \\ v_2 \end{pmatrix} = \frac{1}{m}\left[\begin{pmatrix} R_1 \\ R_2 \end{pmatrix} + \begin{pmatrix} F_1^{\text{ext}} \\ F_2^{\text{ext}} \end{pmatrix}\right]. \tag{1.5}$$

The task is to calculate the interaction forces R_i such that the acceleration will not lead to a violation of the volume exclusion constraint. For example, if both particles are already in
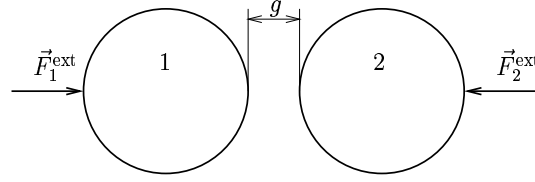
Figure 1.2: Central collision between two non-rotating equal spheres: A simple example for an incipient contact.

contact, their relative velocity must remain zero, i.e. $R_i + F_i^{\text{ext}}$ must be the same for both particles. This is borne out most easily by transforming Newton's equations (1.5) into an equation of motion "of the contact", i.e. of the relative velocity, by using eqs.(1.3) and (1.4):

$$\frac{d\mathcal{V}}{dt} = (-1,1) \cdot \frac{1}{m} \left[\begin{pmatrix} -1 \\ 1 \end{pmatrix} \mathcal{R} + \begin{pmatrix} F_1^{\text{ext}} \\ F_2^{\text{ext}} \end{pmatrix} \right] = \frac{1}{\mathcal{M}} \mathcal{R} + \frac{d\mathcal{V}^{\text{free}}}{dt}. \tag{1.6}$$

In this equation, $\mathcal{M} = m/2$ is the reduced mass of the two particles, and

$$\frac{d\mathcal{V}^{\text{free}}}{dt} = (-1,1) \cdot \frac{1}{m} \begin{pmatrix} F_1^{\text{ext}} \\ F_2^{\text{ext}} \end{pmatrix} = \frac{1}{m}(F_2^{\text{ext}} - F_1^{\text{ext}}) \tag{1.7}$$

would be the relative acceleration without any interaction of the particles.

Solving Eq.(1.6) for $\mathcal{R}$ in the Euler-scheme (1.1) gives the constraint force for the new time step,

$$\mathcal{R}^{\text{new}} = \mathcal{M} \frac{\mathcal{V}^{\text{new}} - \mathcal{V}^{\text{free,new}}}{\Delta t}, \tag{1.8}$$

as a linear function of the relative velocity for the new time step, $\mathcal{V}^{\text{new}}$. Both are unknown and will be determined simultaneously from the constraint conditions. Here and in the following the superscript "new" refers to the value at time $t + \Delta t$, while values of g, $\mathcal{V}$ and $\mathcal{R}$ without this superscript are taken at time t. Note that in the one-contact case worked out here

$$\mathcal{V}^{\text{free,new}} = \mathcal{V} + \frac{1}{m} \left(F_2^{\text{ext}} - F_1^{\text{ext}} \right) \Delta t \tag{1.9}$$

is known.

In addition to Eq.(1.8) one needs the constraint in order to determine the two unknowns, $\mathcal{V}^{\text{new}}$ and $\mathcal{R}^{\text{new}}$. Three conditions must be fulfilled:

- volume exclusion, $g^{\text{new}} = g + \mathcal{V}^{\text{new}} \Delta t \geq 0$,

- contact condition, $g^{\text{new}} \mathcal{R}^{\text{new}} = 0$,

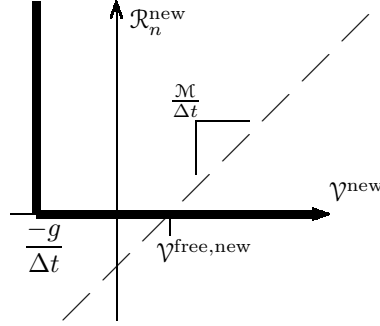- non-cohesiveness (constraint forces purely repulsive), $\mathcal{R}^{\text{new}} \geq 0$.

Figure 1.3: The constraint force $\mathcal{R}^{\mathrm{new}}$ and the relative velocity $\mathcal{V}^{\mathrm{new}}$ for the new time step are related by a Signorini graph (bold line) and by the linear equation of motion (1.8) (dashed line). The intersection of the two graphs determines both values simultaneously.

This means that the set of allowed pairs $(\mathcal{V}^{\mathrm{new}}, \mathcal{R}^{\mathrm{new}})$ is the Signorini graph shown in Fig. 1.3. Its intersection with the linear relation (1.8) determines both values simultaneously. Obviously one gets

$$\mathcal{V}^{\mathrm{new}} = \max\left(-\frac{g}{\Delta t}, \mathcal{V}^{\mathrm{free,new}}\right), \tag{1.10}$$

and

$$
\begin{aligned}
\mathcal{R}^{\mathrm{new}} &= \max\left(0, -\frac{\mathcal{M}}{\Delta t}\left[\frac{g}{\Delta t} + \mathcal{V}^{\mathrm{free,new}}\right]\right) \\
&= \max\left(0, -\frac{\mathcal{M}}{\Delta t}\left[\frac{g}{\Delta t} + \mathcal{V} + \frac{1}{m}(F_2^{\mathrm{ext}} - F_1^{\mathrm{ext}})\Delta t\right]\right).
\end{aligned} \tag{1.11}
$$

This solves the task of calculating the interaction forces R_i, Eq.(1.4), for Newton's equations of motion, Eq.(1.5).

The next section contains the generalization of this to three dimensional space as an easy reference for those who want to write a CD-program. It can be skipped, if one is not interested in the practical algorithmic questions.

1.4 The three dimensional single contact case without cohesion

We consider a pair of rigid particles already in contact or with a small gap between them. They are numbered 1 and 2 and are subject to constant external forces $\vec{F}_1^{\mathrm{ext}}, \vec{F}_2^{\mathrm{ext}}$ acting on the centers of mass (Fig. 1.4). Their restitution coefficient is assumed to be zero. Volume exclusion and Coulomb friction may require a constraint force $\vec{\mathcal{R}}$ at this contact, where we use the convention that $\vec{\mathcal{R}}$ acts on particle 2 while its reaction force $-\vec{\mathcal{R}}$ acts on particle 1. In this section we will show how $\vec{\mathcal{R}}$ is calculated.

Each particle has six degrees of freedom, three translational and three rotational. Accordingly the equations of motion for particle i involve two three component vectors, the center
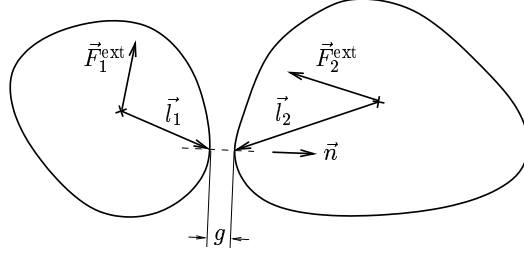
Figure 1.4: Two rigid particles with an incipient contact.

of mass velocity, $\vec{v}_i$, and the angular velocity with respect to the center of mass, $\vec{\omega}_i$. The constraint force $\vec{\mathcal{R}}$ enters the equations of motion for the particle degrees of freedom in terms of interaction forces $\vec{R}_i$ and interaction torques $\vec{T}_i$,

$$\vec{R}_1 = -\vec{\mathcal{R}}\,, \qquad \vec{R}_2 = \vec{\mathcal{R}}\,, \qquad \vec{T}_1 = -\vec{l}_1 \times \vec{\mathcal{R}}\,, \qquad \vec{T}_2 = \vec{l}_2 \times \vec{\mathcal{R}}\,, \tag{1.12}$$

where the vectors $\vec{l}_1$ and $\vec{l}_2$ point from the centers of mass to the expected contact point. (For general particle shapes there may be more than one expected contact point.) It is useful to introduce generalized velocity and force vectors:

$$\mathbf{V} = \begin{bmatrix} \vec{v}_1 \\ \vec{\omega}_1 \\ \vec{v}_2 \\ \vec{\omega}_2 \end{bmatrix}\,, \qquad \mathbf{R} = \begin{bmatrix} \vec{R}_1 \\ \vec{T}_1 \\ \vec{R}_2 \\ \vec{T}_2 \end{bmatrix}\,, \qquad \mathbf{F}^{\text{ext}} = \begin{bmatrix} \vec{F}_1^{\text{ext}} \\ \vec{0} \\ \vec{F}_2^{\text{ext}} \\ \vec{0} \end{bmatrix}\,, \tag{1.13}$$

where $\mathbf{R}$ contains the interaction forces and torques, while $\mathbf{F}^{\text{ext}}$ contains the external forces (external torques are not taken into account here).

As in Eqs.(1.4) and (1.3) the contact quantities $\vec{\mathcal{R}}$ and

$$\vec{\mathcal{V}} = \vec{v}_2 + \vec{\omega}_2 \times \vec{l}_2 - \left(\vec{v}_1 + \vec{\omega}_1 \times \vec{l}_1 \right)\,, \tag{1.14}$$

are linearly related to the corresponding generalized vectors:

$$\mathbf{R} = \mathbf{H}\vec{\mathcal{R}} \tag{1.15}$$
$$\vec{\mathcal{V}} = \mathbf{H}^{\text{T}}\mathbf{V}\,, \tag{1.16}$$

where $\mathbf{H}^{\text{T}}$ is the transpose of the matrix $\mathbf{H}$. These two matrices (defined by Eqs. (1.14) and (1.12)) describe the geometry and allow to transform contact quantities into particle quantities and vice versa.

The equations of motion for the two particles read:

$$\frac{d\mathbf{V}}{dt} = \mathbf{M}^{-1}(\mathbf{R} + \mathbf{F}^{\text{ext}})\,, \qquad \mathbf{M} = \begin{bmatrix} m_1\mathbf{1} & 0 & 0 & 0 \\ 0 & \mathbf{I}_1 & 0 & 0 \\ 0 & 0 & m_2\mathbf{1} & 0 \\ 0 & 0 & 0 & \mathbf{I}_2 \end{bmatrix}\,. \tag{1.17}$$

$\mathbf{M}^{-1}$ is the inverse of the generalized 12×12 mass matrix $\mathbf{M}$, which contains the masses and the matrices of the moments of inertia of the particles ($\mathbf{1}$ denotes the 3×3 unit matrix). In equation (1.17), we neglected a term including the inverse of $d\mathbf{M}/dt$, which takes care of the change of the $\mathbf{I}_i$ due to rotation (and therefore is absent for spheres). For a slowly deforming granular system, this contribution of higher order in $\vec{\omega}$ can be neglected, though. (We will make a similar approximation again in the next paragraph.)

In order to determine the constraint force $\vec{\mathcal{R}}$ and hence the particle interaction $\mathbf{R}$, Eq.(1.15), one transforms Eq. (1.17) into an equation for the relative velocity $\vec{\mathcal{V}}$ by applying $\mathbf{H}^{\mathrm{T}}$ (cf. Eq.(1.6)) (note that the term $(d\mathbf{H}^{\mathrm{T}}/dt)\,\mathbf{V}$ describing the geometrical change is neglected here, which is typically a good approximation) :

$$\frac{d\vec{\mathcal{V}}}{dt} = \hat{\mathcal{M}}^{-1}\vec{\mathcal{R}} + \frac{d\vec{\mathcal{V}}^{\mathrm{free}}}{dt} \ , \tag{1.18}$$

$$\frac{d\vec{\mathcal{V}}^{\mathrm{free}}}{dt} = \mathbf{H}^{\mathrm{T}}\mathbf{M}^{-1}\mathbf{F}^{\mathrm{ext}} \ , \quad \text{and} \quad \hat{\mathcal{M}}^{-1} = \mathbf{H}^{\mathrm{T}}\mathbf{M}^{-1}\mathbf{H} \ . \tag{1.19}$$

$d\vec{\mathcal{V}}^{\mathrm{free}}/dt$ has the meaning of the acceleration without any interaction between the particles, and $\hat{\mathcal{M}}$ denotes the reduced mass matrix of the contact, which replaces the reduced mass in the special case considered in the previous section. It can be shown that $\hat{\mathcal{M}}^{-1}$ acts in a simple way for contacting *spheres* and can be characterized by two parameters m_n and m_t (normal and tangential mass respectively):

$$\hat{\mathcal{M}}^{-1}\vec{\mathcal{R}} \ = \ \frac{1}{m_n}\mathcal{R}_n\vec{n} + \frac{1}{m_t}\vec{\mathcal{R}}_t \ , \tag{1.20}$$

$$\frac{1}{m_n} \ = \ \frac{1}{m_1} + \frac{1}{m_2} \ , \qquad \frac{1}{m_t} = \frac{1}{m_n} + \frac{\vec{l}_1^{\,2}}{I_1} + \frac{\vec{l}_2^{\,2}}{I_2} \ . \tag{1.21}$$

Here the moments of inertia (I_1 and I_2) are numbers and $\vec{n}$ denotes the normal unit vector (perpendicular to the tangent plane), which points from particle 1 towards particle 2. Eq. (1.20) shows that normal and tangential components are not coupled for spheres, which is not true in general.

As in Eq.(1.8) we solve Eq.(1.18) for the contact force and obtain

$$\vec{\mathcal{R}}^{\mathrm{new}} = \hat{\mathcal{M}}\frac{\vec{\mathcal{V}}^{\mathrm{new}} - \vec{\mathcal{V}}^{\mathrm{free,new}}}{\Delta t}, \tag{1.22}$$

where according to Eq.(1.19)

$$\vec{\mathcal{V}}^{\mathrm{free,new}} = \vec{\mathcal{V}} + \mathbf{H}^{\mathrm{T}}\mathbf{M}^{-1}\mathbf{F}^{\mathrm{ext}}\Delta t \tag{1.23}$$

has the meaning of the new velocity if there was no interaction. Now the volume exclusion and non-sliding constraints are used to determine $\vec{\mathcal{V}}^{\mathrm{new}}$, which completes the calculation of the constraint forces (1.22). This is a bit more complicated than in the one-dimensional case and is done in three steps in the algorithm.

1. First we check whether the gap g remains positive after the time step Δt, if the interaction between the particles is not taken into account, i.e. whether

$$g + \mathcal{V}_n^{\mathrm{free,new}}\Delta t > 0 \ . \tag{1.24}$$

The normal component of the relative velocity is given by $\mathcal{V}_n^{\text{free,new}} = \vec{n}^{\text{T}} \cdot \vec{\mathcal{V}}^{\text{free,new}}$. The normal vector $\vec{n}$ is parallel to the shortest connection between the surfaces of the two particles.[1] If condition (1.24) is fulfilled the incipient contact did not close during the time step so that the contact force is zero, $\vec{\mathcal{R}}^{\text{new}} = 0$, and $\vec{\mathcal{V}}^{\text{new}} = \vec{\mathcal{V}}^{\text{free,new}}$. If the left hand side of Eq. (1.24) is zero or negative, the algorithm continues with the second step.

2. In this step the algorithm makes an attempt to establish a non-sliding contact, i.e. we require on one hand that the gap closes:

$$g + \mathcal{V}_n^{\text{new}} \Delta t = 0 \,, \tag{1.25}$$

on the other hand that no slip occurs:

$$\vec{\mathcal{V}}_t^{\text{new}} = 0 \,. \tag{1.26}$$

Therefore the new velocity is $\vec{\mathcal{V}}^{\text{new}} = -(g/\Delta t)\vec{n}$. This determines the contact force Eq.(1.22):

$$\vec{\mathcal{R}}^{\text{new}} = -\frac{1}{\Delta t}\hat{\mathcal{M}}\left(\frac{g}{\Delta t}\vec{n} + \vec{\mathcal{V}}^{\text{free,new}}\right). \tag{1.27}$$

However, this contact force can only be accepted if it lies within the Coulomb cone $|\vec{\mathcal{R}}_t| \leq \mu \mathcal{R}_n$. If this does not hold, we have to give up the assumption of a non-sliding contact. Then the contact will be a sliding one and $\vec{\mathcal{R}}^{\text{new}}$ is recalculated in the third step.

3. For a sliding contact the condition (1.25) remains valid, but Eq. (1.26) does not. Then $\vec{\mathcal{V}}_t^{\text{new}}$ must be determined together with $\vec{\mathcal{R}}_t^{\text{new}}$ from the following condition: The tangential part of

$$\vec{\mathcal{R}}^{\text{new}} = -\frac{1}{\Delta t}\hat{\mathcal{M}}\left(\frac{g}{\Delta t}\vec{n} - \vec{\mathcal{V}}_t^{\text{new}} + \vec{\mathcal{V}}^{\text{free,new}}\right) \tag{1.28}$$

must be equal to sliding friction, i.e.

$$\vec{\mathcal{R}}_t^{\text{new}} = -\mu \mathcal{R}_n^{\text{new}} \frac{\vec{\mathcal{V}}_t^{\text{new}}}{|\vec{\mathcal{V}}_t^{\text{new}}|} \,. \tag{1.29}$$

There are only three unknowns, the normal component of $\vec{\mathcal{R}}^{\text{new}}$ and the tangential components of $\vec{\mathcal{V}}^{\text{new}}$. The three equations (1.28) (one for each component) determine these unknowns.

These three points form a *contact law* that in general provides the contact force in every time step. It can be applied for colliding particles, but also for pre-existing contacts. In this sense no distinction has to be made. Note that this contact law corresponds to a completely

---

[1] This is unique for convex particles. In special cases, e.g. for polygons in two dimensions, a planar contact may form which is modeled by two or more point contacts. Then one should not only consider the shortest connection, but at the same time all other contact-candidates.

inelastic collision, i.e. to zero value of the normal restitution coefficient. To accomplish such a collision, two time steps are needed by this scheme: In the first time step the normal relative velocity is only reduced but it is not set to zero, in order to let the gap close and then in the following time step the relative normal velocity vanishes completely.

Due to practical reasons a slight change is recommended in the contact law [12], that is the application of $g^{\mathrm{pos}} = \max(g, 0)$ instead of g in Eqs. (1.27) and (1.28). This, in principle, makes no difference because g should be non-negative. However, due to inaccurate calculations some small overlaps can be created between neighboring particles. These overlaps would be immediately eliminated by the first version of the inelastic contact law by applying larger repulsive force in order to satisfy Eq. (1.25). This self-correcting mechanism, nonetheless, has the non-negligible drawback that it pumps kinetic energy into the system, when thrusting the overlapping particles away from each other. With the application of g^{pos} one avoids this. Moreover an already existing overlap is not eliminated, only its further growth is inhibited. This can be used to monitor the numerical inaccuracies of a CD-simulation.

For spherical particles the inelastic contact law simplifies, because the reduced mass matrix $\mathcal{M}$ is diagonal for spheres. The three steps are then:

$$
\begin{aligned}
&\text{if} \quad \mathcal{V}^{\mathrm{free}}{}_n \Delta t + g^{\mathrm{pos}} > 0 \\
&\qquad\qquad \text{then} \quad \left\{ \vec{\mathcal{R}}^{\mathrm{new}} = 0 \right. \qquad\qquad\qquad\qquad \text{(no contact)} \\[2mm]
&\qquad\qquad \text{else} \quad \left\{ \begin{aligned} \mathcal{R}_n^{\mathrm{new}} &= -\frac{1}{\Delta t} m_n \left(\frac{g^{\mathrm{pos}}}{\Delta t} + \mathcal{V}_n^{\mathrm{free}} \right) \\ \vec{\mathcal{R}}_t^{\mathrm{new}} &= -\frac{1}{\Delta t} m_t \vec{\mathcal{V}}_t^{\mathrm{free}} \end{aligned} \right. \quad \text{(sticking contact)} \\[3mm]
&\text{if} \qquad \left| \vec{\mathcal{R}}_t^{\mathrm{new}} \right| > \mu \mathcal{R}_n^{\mathrm{new}} \\
&\qquad\qquad \text{then} \quad \left\{ \vec{\mathcal{R}}_t^{\mathrm{new}} = \mu \mathcal{R}_n^{\mathrm{new}} \frac{\vec{\mathcal{R}}_t^{\mathrm{new}}}{\left| \vec{\mathcal{R}}_t^{\mathrm{new}} \right|} \right. \qquad \text{(sliding contact)}
\end{aligned}
$$

$$(1.30)$$

Note, that for a sliding contact the recalculation of $\mathcal{R}_n$ is not necessary in this special case.

Simulations may involve also certain confining objects (e.g. container, fixed wall, moving piston, rotating drum). Therefore the algorithm has to be able to handle not only sphere-sphere contacts, but also sphere-plane and sphere-cylinder contacts. One can easily verify that if planes and cylinders with infinite moments of inertia are used ($I_2 = \infty$), the same simple contact law can be applied as the one derived here for spheres.

1.5 Iterative determination of constraint forces in a multi-contact system

So far we have only discussed how to treat a single incipient or existing contact in the framework of Contact Dynamics. However, the most interesting applications of CD involve dense
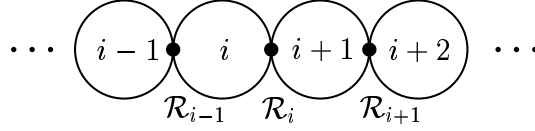
Figure 1.5: A one dimensional array of spheres in contact.

granular media where many particles interact simultaneously within a contact network that may span a substantial part of the whole system.

A simple one-dimensional example is given in Fig. 1.5. Let us assume, that none of the contacts has freshly formed in the last time step, so that all gaps g_i and all relative velocities $\mathcal{V}_i$ are zero, but that the whole array will be accelerated or perhaps disrupted by some external forces acting only on some far away particles of the chain which are not depicted in Fig. 1.5. Eq.(1.11) can be used for the calculation of the constraint force at the i-th contact, but the role of the external forces is now played by the constraint forces of the neighboring contacts. Replacing F_2^{ext} by $-\mathcal{R}_{i+1}^{\text{new}}$ and F_1^{ext} by $\mathcal{R}_{i-1}^{\text{new}}$ in Eq.(1.11) one obtains

$$\mathcal{R}_i^{\text{new}} = \frac{1}{2} \left(\mathcal{R}_{i-1}^{\text{new}} + \mathcal{R}_{i+1}^{\text{new}} \right), \tag{1.31}$$

where we used that the reduced mass is $\mathcal{M} = m/2$ in this simple case and that the right hand side of Eq.(1.31) is ≥ 0. This is a discretized Laplace equation which couples all constraint forces in the contact network.

This example shows that using constraint forces has a serious consequence: A contact force depends also on adjacent contact forces that press the two particles together. Thus for a compressed cluster of rigid particles the contact forces cannot be computed locally. This is a natural consequence of perfect rigidity: As the velocity of sound is infinite, a collision can immediately affect forces even very far away. Whereas in the simple one-dimensional example of Eq.(1.31) the exact calculation of globally consistent constraint forces is feasible, it becomes exceedingly cumbersom for large, complex three-dimensional contact networks. There may even be more than one solution satisfying all constraints [21, 27]. Different algorithms have been used to determine globally consistent constraint forces (e.g. [21, 24]), but in general one uses an iterative scheme (called the *iterative solver*). It is applied in every time step before the implicit Euler integration can proceed one step further with the newly provided forces.

This method works as follows. At each iteration step we update every contact independently in the sense that for one existing or incipient contact a "new" contact force is calculated based on the contact law for the one-contact case, presuming that the current forces of the neighboring contacts were already the correct ones. The resulting force is stored for the given contact and a new contact is chosen for the next update. In that way all the contact forces are updated one by one sequentially. Of course, one update per contact (i.e. one iteration step) does not yet provide a global solution. Such iteration steps have to be repeated many times letting the forces relax according to their neighborhood towards a globally consistent

state. After satisfactory convergence is reached the iteration loop can be stopped. With convergence we mean that further update of the contact forces gives only negligible changes, thus the constraint conditions are practically fulfilled for the whole system. The applied number of iterations N_I within one time step depends on the accuracy of the convergence criterion [2, 26]. Higher N_I provide more accurate forces but require more computational effort.

As an example let us return to the one-dimensional case, Eq.(1.31). If one associates a virtual time step $\Delta t^* = \Delta t/N_I$ with each of the N_I iteration steps performed within a single real time step Δt of the simulation, the forces relax towards a consistent solution of the equations (1.31) according to

$$\frac{\mathcal{R}_i(t^* + \Delta t^*) - \mathcal{R}_i(t^*)}{\Delta t^*} = \frac{N_I}{2\Delta t}\left(\mathcal{R}_{i+1}(t^*) - 2\mathcal{R}_i(t^*) + \mathcal{R}_{i-1}(t^*)\right). \tag{1.32}$$

The change of $\mathcal{R}_i$ per iteration step is equal to the difference between the left and right hand side of the consistency equation (1.31). The virtual time evolution (1.32) is simply a discretized one-dimensional diffusion equation [25] with diffusion constant

$$D \propto N_I \frac{r^2}{\Delta t}, \tag{1.33}$$

where r is the particle radius.

Also in three dimensions, the force consistency with the constraints spreads diffusively during the iteration. For a system of linear size L convergence requires $D\Delta t > L^2 \sim (N^{1/d}r)^2$, where N is the number of particles in the system, which is assumed to be connected throughout, and d is the space dimension. This implies

$$N_I > N^{2/d}. \tag{1.34}$$

The number of iterations needed to reach convergence of the constraint forces for a single time step grows with the number of particles in the system.

When applying the inelastic contact law in three dimensions and replacing $\vec{F}_i^{\text{ext}}$ by the contact forces from neighboring particles, one should not forget that they exert also torques $\vec{T}_1^{\text{ext}}$ and $\vec{T}_2^{\text{ext}}$. They have to be included in the generalized vector $\mathbf{F}^{\text{ext}}$ in Eq.(1.13), where the two torques originally were set to zero.

Regarding the order of the update sequence within the list of (existing and incipient) contacts, it is preferably random and different for each sweep. In this way one avoids any bias in the information spreading. If the update order was from top to the bottom, information would pass faster through the contact network downwards than upwards. It has to be mentioned that the *random sweep* described here differs from the well known *random sequential update*: While in the latter the choice of a contact is independent of the previous choices (the same contact could be selected twice), the *random sweep* selects each contact exactly once within one iteration step. We note that in contrast to this sequential process, a simple parallel update would be unstable.

1.6   Computational effort: Comparison between CD and MD

In this section we estimate the computing time T_{comp} needed for the simulation of a dense N-particle system in d dimensions for a certain real time T_{real}. This gives a certain guidance, for what problems it is advantageous to use Contact Dynamics instead of Molecular Dynamics.

In the derivation of the inelastic contact law (1.30) changes of the matrix $\mathbf{H}$ were neglected. This is only justified if the relative displacement of adjacent particles during one time step is small compared to the particle size and to the radius of curvature of the surfaces in contact. This means that the time step in contact dynamics must be a fraction of r/v, where v is a typical relative velocity and r a typical radius of curvature. Each time step requires $N_I \sim N^{2/d}$ force iterations, each of which takes order N computations. Hence the computational effort for a Contact Dynamics simulation is

$$T_{\text{comp}}^{(\text{CD})} \sim N^{1+2/d} T_{\text{real}} v/r. \tag{1.35}$$

In molecular dynamics with elastic interactions modeled by a linear spring of stiffness K each collision must be time resolved, so that a much shorter time step than in CD is needed. It must be a fraction of the duration of a collision, $\sqrt{m/K}$, where m is the particel mass. The computational effort per time step, however, scales only with the particle number N. Hence

$$T_{\text{comp}}^{(\text{MD})} \sim N T_{\text{real}} \sqrt{K/m}. \tag{1.36}$$

Putting this together we expect

$$\frac{T_{\text{comp}}^{(\text{CD})}}{T_{\text{comp}}^{(\text{MD})}} \sim N^{2/d} \sqrt{\frac{mv^2}{Kr^2}}. \tag{1.37}$$

Systems where this is smaller than 1 can in principle be simulated with CD more efficiently than with MD, see Fig. 1.6.

$\frac{mv^2}{Kr^2}$ is the ratio between a typical kinetic energy per particle and the elastic energy cost to deform a particle substantially, i.e. on the scale of its radius. In most physical situations this factor should be small, because in general the kinetic energy does not suffice to deform collision partners substantially. In particular it is small for quasistatic systems of rigid particles. For such systems it is advantageous to take the limit of infinite rigidity and to use CD instead of MD, provided the particle number is not too large.

The factor $N^{2/d} \propto N_I$ is the price for simulating perfectly rigid particles. For large systems with finite rigidity of the particles, MD costs less computing time than CD. However, if one is willing to use CD with incomplete force relaxation, i.e. with fixed $N_I \ll N^{2/d}$, the CD-algorithm leads to pseudo-elastic behaviour, analogous to soft particle MD-simulations [25]. This involves sound propagation with finite speed and can be described by a damped wave equation. Then $T_{\text{comp}}^{(\text{CD})} \sim T_{\text{comp}}^{(\text{MD})}$.
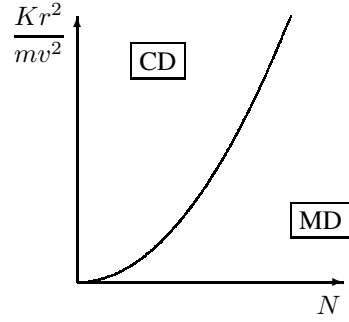
Figure 1.6: Domains where CD, respectively MD simulations are more efficient are separated by a power law $N^{4/d}$.

1.7 Rolling and torsion friction

So far we have characterized the relative motion of two particles by the relative velocity $\vec{\mathcal{V}}$ only. However, their relative orientation can also change, if the relative angular velocity

$$\vec{\Omega} = \vec{\omega}_2 - \vec{\omega}_1 \tag{1.38}$$

is non-zero. A rigid rotation or translation of two arbitrary particles in contact requires $\vec{\mathcal{V}} = 0$ and $\vec{\Omega} = 0$. The first condition means that the particles stay in contact ($\mathcal{V}_n = 0$) and that there is no slip at the contact ($\vec{\mathcal{V}}_t = 0$). The second condition means that there is no torsion ($\Omega_n = 0$) nor rolling motion ($\vec{\Omega}_t = 0$) at the contact.

Torsion and rolling friction are torques $\vec{\mathcal{T}}$ *counteracting* relative angular velocity. They are explained microscopically by forces of different sign acting on opposite sides of a contact region as illustrated in Fig. 1.7. Strictly speaking they are not possible for perfectly rigid particles with a single point contact. However, real particles are not perfectly rigid. Therefore one wants to allow torsion and rolling friction also in the idealized limit considered in Contact Dynamics. Fig. 1.7 shows that the contact torque acts with opposite sign on the angular velocities $\vec{\omega}_i$ of the particles. Therefore one has to replace $\vec{T}_i$ in Eq.(1.12) by

$$\vec{T}_1 = -\vec{l}_1 \times \vec{\mathcal{R}} - \vec{\mathcal{T}}, \quad \vec{T}_2 = \vec{l}_2 \times \vec{\mathcal{R}} + \vec{\mathcal{T}}. \tag{1.39}$$
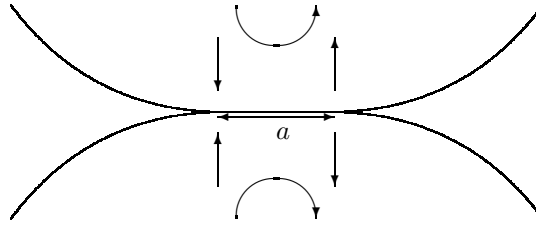

Figure 1.7: An example of forces (vertical vectors) causing rolling friction.

A common heuristic contact law for these rotational degrees of freedom is analogous to Coulomb's friction law, with the relative tangential velocity replaced by the normal respectively tangential components of $\vec{\Omega}$ and friction force replaced by the corresponding components of the contact torque $\vec{\mathcal{T}}$ (Fig. 1.8). Such an ansatz is capable of stabilizing a static heap of spheres on a flat plane [29]. Its implementation in Contact Dynamics is a straight forward generalization of the implementation of Coulomb friction described above (leading to a 6×6 reduced mass matrix $\hat{\mathcal{M}}$).
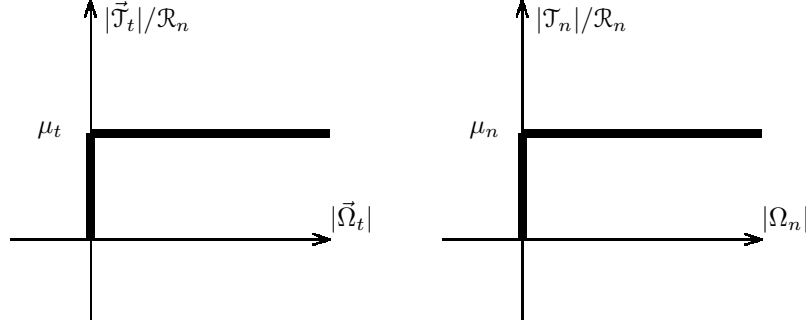

Figure 1.8: Graphs describing rolling friction (left) and torsion friction (right) in contact dynamics.

Recently a rolling friction law was derived based on linear viscoelasticity of the particle material [5, 20]. In contrast to Fig. 1.8 rolling friction vanishes for $\vec{\Omega}_t \to 0$ in that case. As microscopic justification for the heuristic ansatz, Fig. 1.8, one can imagine surface roughness, sinter necks or plastic deformation as origin of rolling friction instead of viscoelasticity. In general one has to expect that the different types of friction are coupled. For sliding and torsion friction this has been worked out [28, 9, 8]: Ignoring the coupling as we do in this paper overestimates friction.

The additional parameters introduced by these contact laws are the coefficients of rolling friction, μ_t, and of torsion friction, μ_n. Unlike their companion μ, they relate *torques* to a force by

$$|\vec{\mathcal{T}}_t| \le \mu_t \mathcal{R}_n, \quad |\mathcal{T}_n| \le \mu_n \mathcal{R}_n \quad , \tag{1.40}$$

therefore bearing the dimension of a length. In the literature of applied physics dealing with rolling friction, this is sometimes obfuscated by considering a wheel of radius R being pushed by a force acting perpendicular to the contact normal $F_{\text{push}} = |\vec{\mathcal{T}}|/R$. Consequently, approximate values for the dimensionless coefficient μ_t/R are provided and turn out to be small compared to μ (confirming that a wheel is indeed a very good idea compared to a sledge).

It is very tempting to presume the length scale contained in μ_t to be proportional to the particle radius r and hence to regard $\overline{\mu} \equiv \mu_t/r$ as a mere material parameter. Assuming furthermore that with two particles of different radii, the geometry enters only via the difference of the particles' curvatures, the corresponding length scale becomes the reduced radius, i.e.

$$\mu_t = r^* \overline{\mu} \tag{1.41}$$

with

$$r^* = \frac{r_1 r_2}{r_1 + r_2} \quad . \tag{1.42}$$

Another classical approach [10] to rolling friction employs rate independent (i.e. non-viscous) hysteretic losses (expressed as a fraction α of the elastic energy put in). In this case

$$|\vec{\mathcal{T}}|_{\max} \sim \alpha a \mathcal{R}_n \quad , \tag{1.43}$$

but the contact diameter a (stemming from the particles' deformation) itself depends on $\mathcal{R}_n$ and (nonlinearly) on r^*, namely according to the Hertz-law

$$a \propto \sqrt{r^* \mathcal{R}_n} \tag{1.44}$$

for discs (or a cylinder on a plane) and

$$a \propto (r^* \mathcal{R}_n)^{1/3} \tag{1.45}$$

for spheres.

An essentially fixed a could also be jusitified, though, in the case of surfaces which exhibit a micro roughness with an amplitude of order $\xi \ll r^*$, providing an $a \sim \sqrt{\xi r^*}$. Else, incorporating (1.43) as a contact law renders the equations of contact dynamics nonlinear.

1.8 Attractive contact forces

Up to now we did not take any kind of attractive interaction between the particles into account. For sufficiently coarse dry granular materials adhesive forces are indeed so weak compared to other forces that this is a good approximation. However for wet granular media and for fine powders adhesion is important. Here we explain how one can include it in Contact Dynamics simulations.
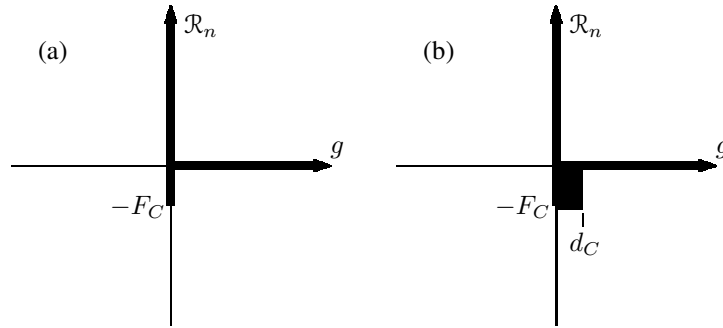

Figure 1.9: Extensions of Signorini's graph to include adhesion: Maximal attractive force F_C at zero distance only (a) and within finite range d_C (b).

While the force/distance-relationship differ for adhesion forces of different origin (van der Waals forces, fluid menisci, . . .), a common characteristic quantity is F_C, the maximal tensile

force the contact can bear. The simplest extension of Signorini's graph is therefore a part of length F_C on the negative force axis as shown in Fig. 1.9(a). Such a zero range attraction is in accordance with the general concept of contact dynamics and, at first sight, seems perfectly reasonable.

However, this would lead to an unphysical behaviour in the limit of vanishing time step Δt. Because of the rigidity of the particles a finite momentum Δp can be transmitted instantaneously, if the connected cluster of particles, to which the contact belongs, collides with some other particle or cluster. This corresponds to a force $\Delta p/\Delta t$ which becomes arbitrarily large if $\Delta t \to 0$. All cohesive contacts with a geometry such that this force acts as a tensile load would open for the slightest shock, if only the time step is chosen small enough. In other words, the principally technical parameter Δt picks up a physical meaning which is highly undesired in numerical simulations.

The missing second ingredient is E_C, the energy needed to separate the two particles. This binding energy is zero in Fig. 1.9(a). The simplest contact law containing nothing else but a cohesion force and a cohesion energy is a constant force F_C up to a distance $d_C \equiv E_C/F_C$ as depicted in figure 1.9(b). A contact can only open, if an external pulling force exceeds the threshold F_C and performs work E larger than E_C so that the particles separate with a kinetic energy $E - E_C$.

The opening of a contact needs usually several time steps, in which the pulling force exceeds F_C. In our implementation a contact which started to open, but not as wide as d_C yet, is not pulled back by the cohesive force, if the tensile load becomes smaller than F_C again. Such a weakened but not yet broken contact can only be strengthened again (closing of the gap), if the particles are pushed together. This simplifies the algorithm and is the reason, why in the graph all pairs of values $(\mathcal{R}_n, g)$ within the rectangle with $0 \leq g \leq d_C$ and $-F_C \leq \mathcal{R}_n \leq 0$ are permitted.

Another question arising with the presence of adhesion is its influence on the friction laws. While various surface effects can be brought into play, the most basic approach is that along the lines of the DMT-model[7] where the attractive force can be considered as an additional external "pushing", i.e. the normal force $\mathcal{R}_n$ in the friction laws has to be replaced by $\mathcal{R}_n + F_C$.

1.9   Conclusion

We tried to give a didactic introduction into the simulation method of Contact Dynamics, pointing also out its strenghts and limitations. The algorithms presented in this article have been applied to investigate the physics of dense granular media by more and more scientists over the last decade, but still Molecular Dynamics is much wider known and often regarded as easier. This does not mean that Contact Dynamics is less powerful, on the contrary. The two techniques have complementary strengths.

We described how to extend the basic algorithm in order to simulate the effects of rolling and torsion friction and of cohesion. Animated examples of these simulations [14] can be found on the CD included in this book. We restricted ourselves to the case, where all particles have zero restitution coefficient. As dense granular media provide an enormous amount of collective dissipation mechanisms due to rearrangements, frustrated rotations etc. a grain hitting such a packing will hardly bounce back: The effective restitution coefficient is close to zero,

which justifies our assumption. How nonzero restitution coefficients could be implemented is described in [19]. Most simulations were done with round particles in two dimensions, but a few simulation results for polygonal particles can be found e.g. in [15]). We are not aware of any Contact Dynamics simulation of polyhedra in three dimensions, although this is certainly feasible, but many cases of incipient contact configurations (corner-face, edge-face, edge-edge etc.) have to be distinguished. Three dimensional simulations of cohesive spheres were done in order to investigate the influence of rolling and torsion friction on the compactibility of porous powders [3].

A nice quantitative validation of the basic Contact Dynamics algorithm can be found in [6], where the experimental shear bands of a packing of parallel rods (a quasi two-dimensional system) could be reproduced in great detail starting the simulation with exactly the same initial configuration. Another stimulating comparison between Contact Dynamics simulations and experiments is presented in [4]. There the uniaxial compaction of porous powders was studied. The key result is a power-law relationship between compacting stress and obtained porosity.

Another active research area, where Contact Dynamics has been successfully applied, are the statistical properties of contact forces in a granular packing under load and their relation to jamming. For example it was shown in [23], that the anisotropic load bearing network of strong force lines is stabilized by the weak forces, which contribute nearly isotropically to the stress. This work was extended in [22] where the role of tensile contact forces between cohesive grains (without rolling friction) was investigated. Finally a topic which is currently intensively studied is the non-uniqueness of realizations of force equilibrium in a dense frictional packing of rigid particles. Contact Dynamics is ideally suited to adress this question [27].

Acknowledgement

Bibliography

[1] D. Baraff. Fast contact force computation for nonpenetrating rigid bodies. In *Computer Graphics Proceedings, SIGGRAPH94*, volume 23, 1994.

[2] G. Bartels. Die Kontakt-Dynamik-Methode. Master's thesis, Gerhard Mercator University, Duisburg, Germany, 2001.

[3] Guido Bartels, Tamás Unger, Dirk Kadau, Dietrich E. Wolf, and János Kertész. The effect of contact torques on porosity of cohesive powders. cond-mat/0403110, submitted to Granular Matter, 2004.

[4] L. Brendel, M. Morgeneyer, D. Kadau, J. Schwedes, and D. E. Wolf. Compaction of cohesive powders: A novel description. In *AIDIC Conference Series, Vol. 6*, pages 55–66. AIDIC & Reed business Information S.p.A., 2003. ISBN 0390-2358.

[5] N. V. Brilliantov and T. Pöschel. Rolling friction of a viscous sphere on a hard plane. *Europhys. Lett.*, 42(5):511–516, 1998.

[6] D. Daudon, J. Lanier, and M. Jean. A micro mechanical comparison between experimental results and numerical simulation of a biaxial test on 2d granular material. In *Powders & Grains 97*, pages 219–222, Rotterdam, 1997. A.A. Balkema.

[7] B.V. Derjaguin, V.M. Muller, and Y.P. Toporov. Effect of contact deformations on the adhesion of particles. *J. Colloid Interface*, 53:314–326, 1975.

[8] Z. Farkas, G. Bartels, T. Unger, and D. E. Wolf. Frictional coupling between sliding and spinning motion. *Phys. Rev. Lett.*, 90:248302, 2003.

[9] S. Goyal, A. Ruina, and J. Papadopoulos. Planar sliding with dry friction. part 2. dynamics of motion. *Wear*, 143:331, 1991.

[10] J.A. Greenwood, H. Minshall, and D. Tabor. Hysteresis losses in rolling and sliding friction. *Proc. Roy. Soc. A*, 259:480–507, 1961.

[11] P. K. Haff. Grain flow as a fluid-mechanical phenomenon. *J. Fluid Mech.*, 134:401, 1983.

[12] M. Jean. The non-smooth contact dynamics method. *Comput. Methods Appl. Mech. Engrg.*, 177:235–257, 1999.

[13] M. Jean and J. J. Moreau. Unilaterality and dry friction in the dynamics of rigid body collections. In *Proceedings of Contact Mechanics International Symposium*, pages 31–48, Lausanne, Switzerland, 1992. Presses Polytechniques et Universitaires Romandes.

[14] D. Kadau. *Porosität in kohäsiven granularen Pulvern und Nano-Pulvern*. PhD thesis, University Duisburg-Essen, Duisburg, Germany, 2004.

[15] D. Kadau, G. Bartels, L. Brendel, and D. E. Wolf. Pore stabilization in cohesive granular systems. *Phase Trans.*, 76(4-5):315–331, 2003. cond-mat/0206572.

[16] P. Lötstedt. Mechanical systems of rigid bodies subject to unilateral contraints. *SIAM J. Appl. Math.*, 42:281, 1982.

[17] S. McNamara and W. R. Young. Inelastic collapse in two dimensions. *Phys. Rev. E*, 50(1):R28–R31, 1994.

[18] J. J. Moreau. Some numerical-methods in multibody dynamics - application to granular-materials. *Eur. J. Mech. A-Solids*, 13:93–114, 1994.

[19] J.J. Moreau. New computation methods in granular dynamics. In *Powders & Grains 93*, page 227, Rotterdam, 1993. Balkema.

[20] T. Pöschel, T. Schwager, and N. V. Brilliantov. Rolling friction of a hard cylinder on a viscous plane. *Eur. Phys. J. B*, 10:169–174, 1999.

[21] F. Radjai, L. Brendel, and S. Roux. Nonsmoothness, indeterminacy, and friction in two-dimensional arrays of rigid particles. *Phys. Rev. E*, 54:861–873, 1996.

[22] F. Radjai, I. Preechawuttipong, and R. Peyroux. Cohesive granular texture. pages 149–162.

[23] F. Radjai, D.E. Wolf, M. Jean, and J.J. Moreau. Bimodal character of stress transmission in granular packings. *Phys. Rev. Lett.*, 80:61–64, 1998.

[24] Th. Schwager and Th. Pöschel. Rigid body dynamics of railway ballast. In *System Dynamics of Long-Term Behaviour of Railway Vehicles, Track and Subgrade*, Berlin, 2002. Springer. Lecture Notes in Applied Mechanics.

[25] T. Unger, L. Brendel, D. E. Wolf, and J. Kertész. Elastic behavior in contact dynamics of rigid particles. *Phys. Rev. E*, 65:061305, 2002. cond-mat/0203575.

[26] T. Unger and J. Kertész. The contact dynamics method for granular media. In *Modeling of Complex Systems*, page 116, Melville, New York, 2003. American Institute of Physics. cond-mat/0211696.

[27] Tamás Unger, Dietrich E. Wolf, and János Kertész. Force indeterminacy in the jammed state of hard disks. cond-mat/0403089, 2004.

[28] K. Voyenli and E. Eriksen. On the motion of an ice hockey puck. *American Journal of Physics*, 53:1149, 1985.

[29] Y. C. Zhou, B. D. Wright, R. Y. Yang, B. H. Xu, and A. B. Yu. Rolling friction in the dynamic simulation of sandpile formation. *Physica A*, 269:536–553, 1999.